

1  
2  
3  
4  
5  
6  
7  
8  
9  
10  
11  
12  
13  
14  
15  
16  
17  
18  
19  
20  
21  
22  
23  
24  
25

Preparation of uniformly-sized alginate microspheres using the novel combined  
methods of microchannel emulsification and external gelation

Ai Mey Chuah<sup>1,2</sup>, Takashi Kuroiwa<sup>2</sup>, Isao Kobayashi<sup>2</sup>, Xian Zhang<sup>1,2</sup>,  
Mitsutoshi Nakajima<sup>1,2,\*</sup>

<sup>1</sup> University of Tsukuba, Graduate School of Life and Environmental Sciences,  
1-1-1 Tennoudai, Tsukuba, Ibaraki 305-8572 Japan

<sup>2</sup> National Food Research Institute, Food Engineering Division,  
2-1-12, Kannondai, Tsukuba, Ibaraki 305-8642 Japan

\* To whom correspondence should be addressed  
Tel: +81-29-853-3981; Fax: +81-29-838-8122  
E-mail: [mnaka@sakura.cc.tsukuba.ac.jp](mailto:mnaka@sakura.cc.tsukuba.ac.jp) (M. Nakajima)

26 **ABSTRACT**

27 The purpose of this study was to prepare alginate (ALG) microspheres with narrow size  
28 distribution using a combination of microchannel (MC) emulsification technique and external  
29 gelation method. ALG solution was dispersed as water-in-oil (W/O) emulsion droplets in iso-  
30 octane containing 5 wt% Span 85 as the immiscible continuous phase via MC emulsification  
31 technique using hydrophobic MC array. The MC array used in this experiment is a grooved-  
32 type MC consisting of 1,070 channels fabricated on a 25 mm x 28 mm silicon microchip. The  
33 monodisperse W/O emulsion droplets generated from the MCs were in the mean particle  
34 diameter ( $d_{av}$ ) range of 18 to 22  $\mu\text{m}$  and coefficient of variation (CV) of 5 to 26% at the ALG  
35 concentrations of 0.5 to 3.0 wt% and flow rates of 0.05 to 0.4 mL/h. The  $d_{av}$  of the emulsion  
36 droplets hardly changed below a dispersed phase threshold flow rate of 0.2 mL/h but  
37 gradually became smaller when the dispersed phase concentration was increased. The  
38 resulting emulsion droplets were then congealed to form rigid ALG gel particles by reacting  
39 them with calcium chloride ( $\text{CaCl}_2$ ) solution. Gelation of the ALG droplets by calcium ion  
40 ( $\text{Ca}^{2+}$ ) resulted in shrinkage of its  $d_{av}$ , forming uniformly-sized ALG microspheres with an  
41 average diameter of 6.2  $\mu\text{m}$  and a CV of below 10% at the ALG concentration of 3 wt%.

42

43 Keywords: Alginate microspheres; Microchannel emulsification; External gelation;  
44 Uniformly-sized emulsion; Water-in-oil emulsion

45

46

47

48

49

50

## 51 **1. Introduction**

52 Hydrocolloid gel particles, for example, alginate (ALG) microspheres have found great  
53 potential in the application of encapsulation of materials such as drugs [1], proteins and  
54 enzymes [2,3], cells [4,5], DNA [6], probiotics [7], flavors [8] and nutrients [9], owing to  
55 their biocompatibility, inert nature, mild encapsulation temperature and high porosity which  
56 allows high diffusion rate of macromolecules.

57 ALG are anionic polysaccharides isolated primarily from brown seaweed. They are  
58 linear, unbranched copolymers of  $\beta$ -D-mannuronic acid (M) and  $\alpha$ -L-guluronic acid (G) units  
59 linked by 1 $\rightarrow$ 4 glycosidic bond with the M- and G- residues distributed as homopolymeric  
60 blocks of M, blocks of G or heteropolymeric blocks of alternating M and G residues [10].  
61 ALG can form gels in the presence of divalent cations such as calcium due to the interchain  
62 binding between G blocks which give rise to a three-dimensional network calcium linked  
63 junctions known as “egg box model” [11].

64 The production of ALG microspheres has traditionally been achieved by extruding an  
65 ALG solution from a needle into a divalent cationic solution to induce gelation [12, 13]. This  
66 relatively mild gelation process has enabled the retention of full biological activity of  
67 proteins, DNA and cells [2]. This method, unfortunately, lacks control over its particle size  
68 and size distribution. The resulting particles might simply be too large or polydisperse to be  
69 deemed efficacious for some practical applications. Reductions in particle size are of critical  
70 importance because the physical properties of the gel particles such as their mechanical  
71 strength, dispersion and mass transfer can be improved vastly while minimizing the rupture  
72 of beads due to gas formation and accumulation [5, 12]. Also, smaller and uniform  
73 microcapsules offer more consistent mechanical properties and the diffusion of oxygen and  
74 nutrients into all area of gel can be better facilitated [13].

75       Recent advances in the state-of-the-art technology of microfabrication have led to the  
76 development of an array of techniques such as membrane emulsification [14], microfluidic  
77 devices [15, 16] and microchannel emulsification [17, 18] capable of producing  
78 monodisperse colloidal particles. In recent years, several groups have attempted to produce  
79 monodisperse ALG microspheres using different microfluidic devices [5, 19] and electric  
80 field application [20]. Nevertheless, the sizes obtained were relatively large, in the range of  
81 50  $\mu\text{m}$  to a few millimeters in size. Though Rondeau and Cooper-White successfully  
82 produced micro and nano sized ALG particles using an axisymmetric flow-focusing  
83 microfluidic device [21], the low concentration of ALG solutions used is a limiting factor in  
84 producing polymeric particles with enhanced structural and mechanical strength.

85       Microchannel (MC) emulsification technique is one of the most promising methods to  
86 produce monodisperse colloidal droplets to date, having been exploited for the production of  
87 a multitude of monodisperse colloidal particles in the size range of 4-100  $\mu\text{m}$  and minimum  
88 CV of less than 5% such as oil-in-water (O/W) emulsion [17, 18, 22], water-in-oil (W/O)  
89 emulsion [17, 23], solid lipid microspheres [24], gel microbeads [25] and giant vesicles [26]  
90 to name a few. Monodisperse emulsion droplets are generated from the MC by permeating a  
91 dispersed phase into a continuous phase through a surface-treated silicon MC with well-  
92 defined geometries [17]. The driving force of the droplet generation is via the spontaneous  
93 transformation of droplets by interfacial tension [27]. This technique is highly energy  
94 efficient because energy loss due to viscous dissipation is very much lower than the  
95 conventional homogenization method which generally releases its energy as heat [28], thus  
96 making it a highly desirable method for the production of emulsions and encapsulation of  
97 highly sensitive compounds prone to destruction during processing.

98       The aim of our study is to use MC emulsification technique to produce uniformly-sized  
99 W/O emulsion droplets with ALG solution as the aqueous phase and then using those

100 emulsion droplets to obtain ALG microspheres via external gelation method with  $\text{CaCl}_2$   
101 solution. The effects of ALG concentration and its flow rate on the size of the W/O emulsion  
102 droplets were also investigated.

103

## 104 **2. Materials and methods**

### 105 2.1 Materials

106 Sodium ALG (viscosity of 80-120 mPa.s in 10 g/L at 20°C), sorbitan trioleate (Span  
107 85), polyoxyethylene sorbitan trioleate (Tween 85) and  $\text{CaCl}_2$  were purchased from Wako  
108 Pure Chemical Industries Ltd. (Osaka, Japan). Iso-octane was obtained from Dojindo  
109 Laboratories (Kumamoto, Japan). Hexamethyldisilazane (LS-7150) was supplied by Shin-  
110 Etsu Chemical Co. Ltd. (Tokyo, Japan) and was used for surface modification of the silicon  
111 MC plate and the glass plate. Milli-Q water was used for the preparation of all aqueous  
112 solutions.

113

### 114 2.2 Formation of uniformly-sized ALG microspheres

115 The preparation of ALG microspheres was based on the modified method of Wan et al.  
116 [29]. The formation of uniformly-sized ALG microspheres involved two separate steps: (1)  
117 preparation of W/O emulsion droplets by MC emulsification and (2) formation of ALG  
118 microspheres by external gelation.

119

#### 120 2.2.1 Preparation of W/O emulsion droplets by MC emulsification

121 Uniformly-sized W/O emulsion droplets were obtained by MC emulsification  
122 technique as described previously by Kawakatsu et al. [30]. Fig. 1a shows the experimental  
123 setup, which consists of a grooved-type hydrophobized silicon plate (EP Tech. Co. Ltd.,  
124 Hitachi, Japan, model CMS 6-1) tightly attached to an optically flat hydrophobized glass

125 plate in the MC module which was initially filled with the continuous phase, two syringe  
126 pumps (Model 11, Harvard Apparatus Inc., MA, USA) to supply the dispersed and  
127 continuous phases, a heating system set at 40°C to provide temperature controlled water  
128 circulation inside the module and a microscope video system to monitor and record the  
129 emulsification behavior. Fig. 1b depicts the grooved MC plate, consisting of 1,070 channels  
130 fabricated on a 25 mm x 28 mm silicon microchip, in which the channel width is 8  $\mu\text{m}$ ,  
131 terrace length is 40  $\mu\text{m}$ , MC depth is 4  $\mu\text{m}$  and well depth is 100  $\mu\text{m}$ . Droplet generation  
132 occurred when the dispersed phase (ALG solution) was forced through the channels into the  
133 continuous phase and was distorted on the terrace, spontaneously transforming them into  
134 spherical droplets (Fig. 1c). The droplets formed were then swept away by the flow of the  
135 continuous phase which was set at 5 mL/h throughout the experiment. A glass plate was  
136 firmly attached to the MC plate to cover the top of the slits on the MC plate and to form  
137 channels between them. The glass and silicon MC plates were treated with a silane coupler  
138 reagent, hexamethyldisilazane to make their surfaces hydrophobic, so that they will be  
139 suitable for the preparation of W/O emulsion according to a modified method by Kawakatsu  
140 et al. [30]. Briefly, the glass and silicon MC plates were plasma oxidized and then soaked in 1  
141 M nitric acid overnight. After washing with water and allowing them to dry, both the glass  
142 and MC plates were dipped in hexamethyldisilazane (100% concentration for MC plate, 20%  
143 in hexane for glass plate) and left for 2 nights at room temperature. Finally, the unreacted  
144 materials were washed away.

145 ALG solutions at varying concentrations (0.1 to 3.0 wt%) were prepared by dissolving  
146 ALG powder in Milli-Q water at 60°C for at least 2 hours. After storing the solutions at 4°C  
147 overnight to ensure complete hydration, the solutions were then maintained at 40°C (which is  
148 the emulsification temperature) before being used as the dispersed phase. The continuous  
149 phase consisted of Span 85 at a concentration of 5 wt% dissolved in iso-octane. In order to

150 improve the stability of the W/O emulsion and to prevent diffusion of the ALG droplets into  
151 the organic phase, iso-octane was pre-treated prior to use as follows: Span 85 in iso-octane  
152 was saturated with water by allowing it to come into contact with water at a volume ratio of  
153 9:1 (iso-octane:water) for 30 min, after which they were separated by centrifugation at 1200 x  
154 g for 15 min using a table centrifuge (KN-70, Kubota, Tokyo, Japan). The iso-octane  
155 supernatant part was used as the continuous phase [26].

156 The MC plate used for producing W/O emulsion in this experiment was cleaned using  
157 an ultrasonic bath (VS-100III, As One Co., Osaka, Japan) at a frequency of 45 kHz based on  
158 the following sequences: MC plate was cleaned in Milli-Q water for the first 20 min followed  
159 by Milli-Q water containing a non-ionic detergent for another 20 min, Milli-Q water  
160 containing ethanol (1:1 v/v proportion) for the next 20 min and another round of cleaning  
161 with Milli-Q water for the final 20 min. The MC plate was then left to dry in an oven at 60°C  
162 before use.

163

#### 164 2.2.2 Formation of alginate microspheres by external gelation

165 Prior to the external gelation process, the W/O emulsion ( $\sim 3.6 \times 10^4$  droplets/mL) was  
166 diluted with iso-octane solution to a final Span 85 concentration of 2.3 wt% ( $\sim 1.7 \times 10^4$   
167 droplets/mL). Estimation of the number of droplets in the emulsion was based on the  
168 calculations made according to the amount of solubilized water in the continuous phase  
169 measured using the E-684 Karl Fisher Coulometer (Metrohm, Herisau, Switzerland). A  
170 solution containing 0.12 g Tween 85 in 0.54 g iso-octane was added to 5 g of the diluted  
171 emulsion and mixed gently with a stirrer for 5 min. Subsequently, 1.3 mL of 10 % aq. CaCl<sub>2</sub>  
172 solution was added into the emulsion to start the gelation process. After gentle mixing for 20  
173 min, the resulting ALG microspheres were rinsed three times with Milli-Q water by

174 successive centrifugation cycles (300 rpm, 10 min) and stored in Milli-Q water at room  
175 temperature.

176

### 177 2.3 Determination of particle diameter

178 The particle diameter of the emulsion droplets and microspheres were determined by  
179 measuring the diameter of the captured images of over 200 particles using an image  
180 processing software (Winroof, Mitani Co., Fukui, Japan). The coefficient of variation (CV)  
181 was calculated based on the following equation:

$$182 \text{ CV} = (\sigma / d_{\text{av}}) \times 100$$

183 where  $\sigma$  is the standard deviation and  $d_{\text{av}}$  is the mean particle diameter.

184

### 185 2.4 Microscopy observation

186 The morphologies of some selected emulsions and ALG microspheres were observed  
187 using a light microscope (Leica DM IRM; Leica Microsystems Wetzlar GmbH, Germany). A  
188 drop of the sample was placed on a microscope slide and covered with a cover slip.  
189 Photomicrography images of the samples were captured using digital image processing  
190 software (Canopus Co. Ltd., Japan).

191

### 192 2.5 Determination of viscosity

193 The viscosities of both the dispersed phase and continuous phase containing 5 wt% Span 85  
194 were measured using a vibrational viscometer (SV-10, A&D Company Ltd. Tokyo, Japan) at  
195 25°C. Vibrational viscometer measures viscosity by detecting the electromagnetic electric  
196 current necessary to resonate the two sensor plates (immersed in the fluid sample whose  
197 viscosity is to be determined) at a constant frequency and amplitude. The driving electric  
198 current will be detected as the magnitude of viscosity produced between the sensor plates and

199 the fluid sample. The viscosity measured was then calculated to obtain the absolute viscosity  
200 based on the following formula:

$$201 \quad \text{Absolute viscosity} = \text{viscosity measured} / \text{density}$$

202 The absolute viscosity value was referred simply as viscosity throughout the manuscript.  
203 Each measurement was repeated five times and the calculated mean values were used.

204

## 205 2.6 Determination of interfacial tension

206 The interfacial tension between an ALG solution (0 to 3 wt%) and the continuous phase  
207 was determined by using the pendant drop method. The profile of the drop of ALG solution  
208 suspended in 5 wt% Span 85 was measured using a full automatic interfacial tensiometer  
209 (PD-W, Kyowa Interface Science Co., Ltd., Saitama, Japan). Each measurement was repeated  
210 at least 20 times and the calculated mean values were used.

211

## 212 2.7 Determination of contact angle

213 The static contact angle in this study was defined as the angle of the ALG solution  
214 droplet to the MC plate surface in the continuous phase. These contact angles were measured  
215 by analyzing the images captured of the ALG solution droplets after the shape of the ALG  
216 solution droplets became stable on the MC plate surface. Each measurement was repeated at  
217 least five times and the calculated mean values were used.

218

# 219 3. Results and discussion

## 220 3.1 Preparation of W/O emulsion droplets by MC emulsification

221 W/O emulsion droplets were used as precursors for the formation of uniformly-sized  
222 ALG microspheres. Kawakatsu et al. first proposed the production of monodisperse W/O  
223 emulsions using hydrophobic grooved MC arrays, which consisted of highly uniform micro-

224 grooves with a slit-like terrace and a deeply etched well [17]. Fig. 2 shows the successful MC  
225 emulsification of uniformly-sized W/O emulsion droplets with 3 wt% ALG solution as the  
226 dispersed phase (flow rate of 0.05 mL/h) and 5 wt% Span 85 in iso-octane as the continuous  
227 phase (flow rate of 5 mL/h). It has been suggested that a low hydrophilic-lipophilic-balance  
228 (HLB) value of the surfactant was necessary to produce stable W/O emulsions by MC [23].  
229 The surfactant used in our experiment, Span 85, has an HLB value of 1.8 and was found to be  
230 capable of forming stable W/O emulsions. During droplet generations, the dispersed phase  
231 passed through the channels and began to expand in a disk-like shape at the terrace which  
232 continued to expand in the well and subsequently detached from the well. The domineering  
233 force of the spontaneous transformation of the to-be-dispersed phase can be explained by the  
234 interfacial tension effects on the terrace and in the well due to the instability and nonlinearity  
235 flow of the to-be dispersed and continuous phases [31]. Microscopic observation of the  
236 sample withdrawn from the dispersions before the addition of  $\text{CaCl}_2$  revealed a morphology  
237 that is uniformly-sized, discrete and spherical. The surfaces of the MC plate and glass plate  
238 which were initially hydrophilic (due to the presence of silanol groups on their surface) were  
239 modified by hexamethyldisilazane to make them hydrophobic. After silanization, the static  
240 contact angles of the ALG solutions on the surface of the modified MC plate were measured  
241 to be approximately  $145^\circ$ - $150^\circ$  across the various ALG concentration studied (from 0.1 wt%  
242 to 3 wt%), indicating that the difference in the ALG concentrations did not have a remarkable  
243 effect on the contact angles (Table 1). Sugiura et al. and Kawakatsu et al. reported that when  
244 the contact angles were greater than  $120^\circ$ , W/O emulsions were successfully generated from  
245 the MCs and these contact angles were found to be dependent on the composition of the oil  
246 phase (i.e. the continuous phase of W/O emulsion), the type of surfactant and silane coupler  
247 reagent used for the modification of the MC surface [23, 30]. Furthermore, these large  
248 contact angles were also an indication of the preferential wetting of the channel surface by

249 the continuous phase, which is another important prerequisite for the successful generation of  
250 uniformly sized droplets [17, 30].

251

### 252 3.2 Effect of ALG concentration in dispersed phase

253 Other factors have also been identified to affect droplet formation, such as channel  
254 geometry, composition of the to-be-dispersed phase and continuous phase and types of  
255 surfactants/emulsifiers [32-34]. The viscosity ratio of dispersed phase to continuous phase  
256 has also been indicated to be another determining factor influencing the formation time and  
257 size of emulsion droplets [30, 35]. In our experiment, the effect of dispersed phase  
258 concentration on the  $d_{av}$  and CV of the W/O emulsion was investigated (Fig. 3a). The  
259 viscosity of the ALG solution, as expected, increased with higher ALG concentration while  
260 the interfacial tension at the interface of the ALG solution (concentration of 0.1 wt% to 3.0  
261 wt%) and continuous phase remained almost unchanged (Table 1). The flow rates of the  
262 dispersed and continuous phases were controlled at 0.05 mL/h and 5 mL/h respectively.  
263 When the ALG concentration was increased, the  $d_{av}$  and the CV of the emulsion droplets  
264 decreased from ca. 22  $\mu\text{m}$  to 18  $\mu\text{m}$  and 26% to 5% respectively (Fig. 3a). These results  
265 correlated well with its particle size distribution which became narrower as the ALG  
266 concentration was increased, indicating the formation of a more regular W/O emulsion  
267 droplets (Fig. 3b). Kawakatsu et al. [30] demonstrated a decrease in the  $d_{av}$  when the ratio of  
268 the viscosity of the dispersed phase to the continuous phase increased. As the viscosity of the  
269 dispersed phase increased, the rate in which the dispersed phase was transferred to the terrace  
270 became slower, causing the amount of the dispersed phase supplied into the well and  
271 subsequently the channel exit to decrease [30, 35], hence explained the smaller  $d_{av}$  obtained  
272 in our experiment. Kobayashi et al. reported that a decrease in the droplet diameter of SDS  
273 stabilized O/W emulsion droplets produced via the oblong MCs was influenced by the

274 increase in the dispersed phase (silicone oil) viscosity at below the threshold level of 100  
275 mPa. On the other hand, they attributed the increase in the droplet diameter above the  
276 threshold level to the reduction in the dynamic interfacial tension [36].

277 A study by Sugiura et al. revealed that a low to-be-dispersed phase viscosity during MC  
278 emulsification will lead to an increase in the production rate of droplets from each channel  
279 [35]. However, this was apparently not the case in our study as droplet formation from the  
280 channels proved to be difficult at low dispersed phase viscosity (i.e. ALG concentration of  
281 0.1 wt%). At the start of the emulsification process, the dispersed phase appeared to have  
282 flowed through the channels and reached the channel exits. However, very few droplets were  
283 generated as almost no channels were functioning except for a few channels (Fig. 4a). These  
284 active channels too soon stopped working shortly after the droplets were formed. Emulsion  
285 droplets could only be generated again from the MCs when more force was applied to the  
286 dispersed phase flow. Once this force was removed, droplets generation from the channels  
287 stopped instantly, concurrently with the withdrawal of the dispersed phase back into the  
288 narrow channels.

289 A close look at these channels showed some small aggregates consisting of tiny  
290 droplets accumulating at the channel cleavage and blocking the outflow of the dispersed  
291 phase from the channel exits. These aggregates could also be seen to form a layer on the  
292 surface of some of the freshly formed droplets under low ALG emulsification condition (Fig.  
293 3c). However, when sodium chloride (~0.5 wt%) enriched ALG solution was used as the  
294 dispersed phase, no aggregates were observed and emulsion droplets could be formed easily  
295 even without exerting extra pressure to the dispersed phase. Similar observations were also  
296 noted by Kobayashi et al. who studied the effect of osmotic pressure of the pure and salted  
297 water dispersed phase on the formation behavior of W/O emulsion through an asymmetric  
298 straight-through MC array [37]. They reported the formation of highly uniform aqueous

299 droplets at an osmotic pressure of 0.42 MPa and above but at a low osmotic pressure (i.e.  
300 0.085 MPa and below), droplets formed were polydisperse and were marked by the presence  
301 of a rough thin layer surrounding the droplets, in correlation to our observation as mentioned  
302 earlier. They suggested this to a phenomenon known as “spontaneous emulsification (SE)”,  
303 which occurred at the interface between two liquids under a favorable condition.

304 In order to confirm this phenomenon, the following experiment was carried out to  
305 mimic the behavior of the emulsion droplets in the continuous phase. A small drop of the  
306 dispersed phase (0.1 wt% ALG concentration) measuring about 1 mm in diameter was  
307 carefully dispensed from a syringe needle and allowed to hang in the continuous phase while  
308 making sure that the drop did not detach from the tip of the needle during the course of the  
309 experiment. Changes to the interface of the drops were observed over time (Fig. 4b(i)). At the  
310 start of the experiment, the surface of the drop was clearly smooth (0 min). As time evolved,  
311 a whitish layer (which appeared to be aggregates of small droplets) surrounding the bottom  
312 portion of the drop started to become visible (15 min). This whitish layer continued to grow  
313 over time until it completely covered the whole drop (30 min) and finally formed a rough  
314 contour of aggregates around the drop (45 min). The growth of the observed whitish layer is  
315 evidently consistent with the behavior of SE. Uricanu et al. in their study on SE behavior at  
316 the water-oil interfaces with pure or salted water or gelatin solutions as the aqueous phase  
317 and Span 80 in dodecane as the oil phase, discovered the formation of sparse small droplets  
318 that increased in number and size over time until the concentration gradients between the oil  
319 phase and water-oil interface reached equilibrium [38]. SE can only occur at above a  
320 surfactant threshold concentration [38] and in our study, the Span 85 at a concentration of 5  
321 wt% was more than sufficient to induce SE especially at low ALG concentration.  
322 Nevertheless, at higher ALG concentration, for example 2.0 wt%, while keeping the  
323 concentration of surfactant constant, the process of SE was somewhat delayed or inhibited as

324 the drop surface appeared to be smooth throughout the duration of the experiment (Fig.  
325 4b(ii)), a result which was similar to the observation during MC emulsification.

326 The presence of other components (e.g. salt or gelatin) in the aqueous phase has been  
327 shown to suppress SE though not likely to arrest the process completely [38]. The presence of  
328 sufficiently high ALG concentration in the aqueous phase in our study was believed to have  
329 exerted the same effect of protecting the interface against SE. The mechanisms that is  
330 responsible for SE is still not very well understood. It has been reported that electrolyte such  
331 as potassium chloride, when added to the dispersed phase act as a stabilizer for W/O  
332 emulsion droplets [39]. The presence of additives like salt will create an osmotic pressure in  
333 the water phase, forcing the surfactant to compete with the salt and interfering in the mass  
334 transport of water molecules across the water-oil interface [38]. Therefore, in enriched  
335 aqueous phase (with salt or gelatin), a higher surfactant concentration would be needed to  
336 induce SE [38]. Also, as a result of preferential hydration of salt, a decrease in the interaction  
337 between water molecules and the hydrophilic group of surfactant molecules at the interface of  
338 the water-oil could have also strongly suppressed SE [40].

339 Though the presence of salt in one way will aid in the inhibition of SE, their presence  
340 will also result in an ALG gel structure which is physically unstable and weak such as when  
341 the anti-gelling cation of sodium and magnesium ions or chelating agents are used [7].  
342 Considering all these factors, the most strategic resolution would be to produce the emulsion  
343 using a higher ALG concentration to avoid the incorporation of salt in the aqueous phase.  
344 Moreover, ALG particles made from high viscosity ALG solutions will impart the gel  
345 structure which is mechanically and physically more superior due to an increase in the  
346 polymer chain density and entanglement [4, 13].

347

348 3.3 Effect of flow rate of dispersed phase

349 In order to investigate the effect of flow rate of the dispersed phase on the  $d_{av}$  and its  
350 CV, the flow rate of the ALG solution was varied from 0.05 mL/h to 0.4 mL/h with the  
351 continuous phase flow rate fixed at 5 mL/h and ALG concentration kept constant at 3 wt%.  
352 We did not study the effect of the continuous phase flow rate as it has been reported  
353 previously that its influence was minimal [41]. Figs. 5a and 5b show changes in the  $d_{av}$ , CV  
354 and particle size distribution of the O/W emulsion droplets as a function of the dispersed  
355 phase flow rate. At a dispersed phase flow rate of 0.2 mL/h and below, the  $d_{av}$  of the W/O  
356 emulsion droplets was measured to be consistently the same at 18  $\mu\text{m}$  but at a flow rate above  
357 0.2 mL/h, a slight increase in the  $d_{av}$  was observed (Fig. 5a). During droplet formation, the  
358 formation of larger  $d_{av}$  at a higher dispersed phase flow rate could be attributed to the increase  
359 in the volume of the dispersed phase that flowed into the well as the dispersed phase flow rate  
360 was increase. Nevertheless, the CV remained almost constant and the change in  $d_{av}$  was in  
361 fact not as pronounced as the one encountered when the ALG concentration was increased.  
362 Kobayashi et al. revealed that when soy bean oil or silicone oil was used as the dispersed  
363 phase and 1.0 wt% SDS was used as the continuous phase, the size of the droplet diameter of  
364 O/W emulsions was independent of the dispersed phase flow rate at below a threshold level  
365 but above this critical level, the increase in the droplet size was highly dependent on the  
366 dispersed phase velocity inside the channel [42]. Sugiura et al. noted that the increase in the  
367  $d_{av}$  as attributed to an increase in the dispersed phase flow rate was especially more obvious  
368 when the viscosity of the continuous phase was higher (e.g. in tetradecane or hexadecane) but  
369 to a lesser extent when a lower viscosity continuous phase was used (e.g. octane or decane)  
370 due to the longer duration taken to form droplets at the former [23].

371 Fig. 5c shows the droplet productivity at different flow rates of the dispersed phase  
372 based on the calculation of the  $d_{av}$ . The rate of increment in droplet productivity was  
373 especially more conspicuous at the flow rates of 0.2 mL/h and below because the  $d_{av}$  obtained

374 remained relatively unchanged even with an increase in the flow rates of the dispersed phase.  
375 In fact, droplet productivity at these flow rates can be expressed by the following simple  
376 linear equation:

$$377 \quad f = 3.2 \times 10^8 Q_d$$

378 where  $f$  is the droplet productivity (number of droplets/h) and  $Q_d$  is the flow rate of alginate  
379 solution (mL/h). In contrast, above these flow rates, the rate of increment in their droplet  
380 productivity was less pronounced due to the formation of droplets with larger volume marked  
381 by higher flow rates.

382

### 383 3.4 Formation of ALG microspheres by external gelation

384 Prior to external gelation, Tween 85 was added to the W/O emulsion followed  
385 subsequently by the addition of CaCl<sub>2</sub> to induce gelation. At the ALG concentration of 3  
386 wt%, shrinkage of the ALG gel particles by approximately 96% (volume basis) from the  
387 initial W/O  $d_{av}$  of 18.1  $\mu\text{m}$  prior to gelation (Fig. 6a(i)) to ca. 6.2  $\mu\text{m}$  of ALG microspheres  
388 after gelation (Fig. 6a(iv)) was observed. The ALG microspheres obtained appeared to be  
389 highly spherical and uniform in size with no visible imperfections or irregularities at a CV of  
390 below 10%. The decrease in particle size was supported by the particle size distribution  
391 which showed a shift of its size distribution from the upper size range to the lower size range  
392 (Fig. 6b).

393 The addition of the right blend of a lipophilic surfactant (i.e Span 85) and a hydrophilic  
394 surfactant (i.e Tween 85) has been reported to improve droplet dispersity [43], hence  
395 facilitate the formation of a more stable emulsion. In addition, the incorporation of sufficient  
396 quantities of the surfactants are essential to ensure that the particles formed are discrete and  
397 spherical in shape and not distorted or fused together in large aggregates [44]. Also, the  
398 hydrophile-lipophile balance (HLB) of the surfactant mixture has been found to affect the

399 size distribution, shape and drug release profile of the ALG microspheres [29]. Fig. 6a shows  
400 the microscopy images of the W/O emulsion before external gelation and ALG microspheres  
401 after external gelation. The ALG microspheres were subjected to different concentration  
402 ratios of the surfactants in order to optimize the best condition for the formation of discrete  
403 and uniformly-sized ALG microspheres. Both Tween 85 and Span 85 are non-ionic  
404 surfactants with HLB values of 11.0 and 1.8 respectively. In the absence of Tween 85  
405 (concentration ratio of Tween 85 to Span 85 of 0), microspheres obtained were highly  
406 aggregated (Fig. 6a(ii)). However when Tween 85 was incorporated into the system at a  
407 concentration ratio of 0.5, the aggregation appeared to be less pronounced (Fig. 6a(iii)).  
408 Nevertheless, in both cases, it was difficult to disperse the aggregated droplets by water bath  
409 sonication. At a higher Tween 85 to Span 85 concentration ratio of 1.0 (equivalent to higher  
410 HLB value), the microspheres obtained were dispersed as discrete spherical particles (Fig.  
411 6a(iv)). In the event of some slight flocculations, we were able to separate these flocs into  
412 discrete particles by subjecting the particles to sonication while maintaining its uniformity.  
413 Wan et al. suggested that surfactant mixture with a higher HLB value (equivalent to a higher  
414 proportion of the hydrophilic surfactant) has a greater affinity for  $\text{CaCl}_2$  [44], and hence  
415 would be able to form rigid microspheres completely before they could be distorted by the  
416 turbulence resulting from introducing  $\text{CaCl}_2$  solution into the system. Therefore, the right  
417 proportion of the two surfactants is critical in order to obtain ALG particles with the desired  
418 attributes. Other factors indicated to have pronounced influences on the size and morphology  
419 of the ALG microspheres were stirring speed, rate of  $\text{CaCl}_2$  addition, concentration and  
420 composition of encapsulating material [43].

421  $\text{CaCl}_2$  acts as a cross-linking agent, whereby the positively charged  $\text{Ca}^{2+}$  ions form  
422 electrostatic bridges between the negatively charged polysaccharides [45]. These divalent  
423 cations participated in the intermolecular binding between the relatively stiff G-blocks on

424 different ALG molecules by forming junction zones which resulted in a three dimensional  
425 network gel. The binding zone between G-blocks is commonly known as the “egg-box  
426 model” [11].  $\text{CaCl}_2$  would initially react with sodium alginate on the surface of the particles,  
427 enveloping the liquid particles with a thin layer of calcium alginate. The gradual diffusion of  
428  $\text{CaCl}_2$  into the core of the particles would eventually congeal the liquid core into rigid  
429 microparticles [43].

430 It is also well established that calcium–alginate gels shrink during gel formation due to  
431 water loss [46]. The kinetics of shrinkage may not solely lie with the gelation process as  
432 described above but may also be attributed to the process prior to gelation ie. during the MC  
433 emulsification process. Rondeau and Cooper-White attributed the size reduction of the ALG  
434 droplets during their transport downstream along the microfluidic channel to loss of water  
435 due to diffusion out of the polymeric droplets as a result of its partial miscibility with the  
436 continuous phase (which consists of anhydrous dimethyl carbonate) [21]. Presumably, the  
437 same phenomena occurred in our system, the diffusion of water at the interface of the two  
438 phases ie. the ALG and the Span 85-containing iso-octane phases are expected to proceed till  
439 both phases are in equilibrium with respect to each other. There is a possibility that the  
440 solvent exchange process could have taken place simultaneously with the gelation process  
441 unless the above mentioned equilibrium process is reached before the cross-linking process.  
442 Otherwise, the diffusion of the ALG phase would only stopped when it reached a stage in  
443 which the gel particles became condensed and finally hardened. Therefore, the relative  
444 solvency of the two liquids plays an important role in determining the rate of diffusion. This  
445 competing kinetics would have been one of the determining factors affecting its particle size.  
446 In addition, an increase in the  $\text{Ca}^{2+}$  content has also been widely known to cause greater  
447 shrinkage due to enhanced crosslinking density [13]. The degree of shrinkage has also been  
448 reported to be affected by the initial ALG concentration in the solution with a higher

449 concentration contributing to a much smaller and slower volume loss [21]. For example, we  
450 noticed that the W/O emulsion droplets produced at 0.1 wt% ALG concentration completely  
451 disappeared (based on our unaided eye observation) after leaving them overnight. In contrast,  
452 the presence of emulsion droplets was still evident after overnight when the concentration of  
453 ALG used was greater.

454

#### 455 **4. Conclusions**

456 Uniformly-sized ALG microspheres were successfully fabricated using the combined  
457 MC emulsification technique and external gelation method. The formation of uniformly-sized  
458 W/O emulsion by MC emulsification preceded the formation of ALG microspheres.  
459 Emulsion droplets formed were between 18 to 22  $\mu\text{m}$  at ALG concentration of 0.5% to 3.0  
460 wt% and flow rate of 0.05 to 0.4 mL/h. Droplet generation appeared to be difficult at low  
461 ALG concentration (i.e. 0.1 wt%), probably as a result of the spontaneous emulsification (SE)  
462 phenomenon. Nevertheless, the smallest  $d_{av}$  and lowest CV of the W/O emulsions were  
463 obtained when the dispersed phase viscosity was at its highest while the flow rate of the  
464 dispersed phase was at the lowest. The  $d_{av}$  and CV of the ALG microspheres prepared at an  
465 ALG concentration of 3 wt% upon gelation was ca. 6.2  $\mu\text{m}$  and below 10% respectively.

466

#### 467 **Acknowledgement**

468 This work was supported in part by the Food Nanotechnology Project of the Ministry of  
469 Agriculture, Forestry and Fisheries of Japan.

470

#### 471 **References**

- 472 [1] A.D. Sezer, J. Akbuga, Release characteristics of chitosan treated alginate beads: II.  
473 Sustained release of a low molecular drug from chitosan treated alginate beads, J.  
474 Microencapsulation 16 (1999) 687-696.
- 475 [2] W.R. Gombotz, S. F. Wee, Protein release from alginate matrices. Adv. Drug Delivery  
476 Rev. 31 (1998) 267-285.
- 477 [3] A.R. Degroot, R.J. Neufeld, Encapsulation of urease in alginate beads and protection  
478 from  $\alpha$ -chymotrypsin with chitosan membranes, Enzyme Microbial Tech. 29 (2001) 321-  
479 327.
- 480 [4] O. Smidsrød, G. Skjåk-Bræk, Alginate as immobilization matrix for cells. Trends  
481 Biotech. 8 (1990) 71-78.
- 482 [5] S. Sugiura, T. Oda, Y. Aoyagi, R. Matsuo, T. Enomoto, K. Matsumoto, T. Nakamura, M.  
483 Satake, A. Ochiai, N. Ohkohchi, M. Nakajima, Microfabricated airflow nozzle for  
484 microencapsulation of living cells into 150 micrometer microcapsules, Biomed.  
485 Microdevices 9 (2007) 91-99.
- 486 [6] D. Quong, R.J. Neufeld, DNA protection from extracapsular nucleases, within chitosan-  
487 or poly-L-lysine-coated alginate beads, Biotech. Bioeng. 60 (2000) 134-134.
- 488 [7] J.S. Lee, D.S. Cha, H.J. Park, Survival of freeze-dried *Lactobacillus bulgaricus* KFRI  
489 673 in chitosan-coated calcium alginate microparticles, J. Agric. Food Chem. 52 (2004)  
490 7300-7305.
- 491 [8] A.H. King, Flavour encapsulation with alginates, in: S.J. Risch, G.A. Reineccius (Eds.),  
492 Flavour Encapsulation, American Chemical Society, Washington, 1988, pp. 122-125.
- 493 [9] K.G.H. Desai, C. Liu, H.J. Park, Characteristics of vitamin C immobilized particles and  
494 sodium alginate beads containing immobilized particles, J. Microencapsulation, 22  
495 (2005) 363-376.

- 496 [10] K.I. Dragnet, Alginates, in: G.O. Phillips, P.A. Williams (Eds.), Handbook of  
497 Hydrocolloids, CRC Press, Boca Raton, FL, 2000, pp. 381-383.
- 498 [11] G.T. Grant, E.R. Morris, D.A. Rees, P.J.C. Smith, D. Thom, Biological interactions  
499 between polysaccharides and divalent cations: the egg-box model. FEBS Lett. 32 (1973)  
500 195-198.
- 501 [12] D. Poncelet, R. Lencki, C. Beaulieu, J.P. Halle, R.J. Neufeld, A. Fournier, Production of  
502 alginate beads by emulsification/internal gelation. I. Methodology. Appl. Microbio.  
503 Biotechnol. 38 (1992) 39-45.
- 504 [13] C.K. Kuo, P.X. Ma, Ionically crosslinked alginate hydrogels as scaffolds for tissue  
505 engineering: Part 1. Structure, gelation rate and mechanical properties, Biomaterials 22  
506 (2001) 511-521.
- 507 [14] T. Nakashima, M. Shimizu, M. Kukizaki, Particle control of emulsion by membrane  
508 emulsification and its application, Adv. Drug Deliver Rev. 45 (2000) 47-56.
- 509 [15] T. Thorsen, R.W. Roberts, F.H. Arnold, and S.R. Quake, Dynamic pattern formation in a  
510 vesicle-generating microfluidic device, Phys. Rev. Lett. 86 (2001) 4163-4166.
- 511 [16] D.R. Link, S.L. Anna, D.A. Weitz, H.A. Stone, Geometrically mediated breakup of  
512 drops in microfluidic devices, Phys. Rev. Lett. 92 (2004) 054503.1-054503.4.
- 513 [17] T. Kawakatsu, Y. Kikuchi, M. Nakajima, Regular-sized cell creation in microchannel  
514 emulsification by visual microprocessing method. J. Am. Oil Chem. Soc. 74 (1997) 317-  
515 321.
- 516 [18] I. Kobayashi, S. Mukataka, M. Nakajima, Novel asymmetric through-hole array  
517 microfabricated on a silicon plate for formulating monodisperse emulsions, Langmuir,  
518 21 (2005) 7629-7632.

- 519 [19] K.S. Huang, T.H. Lai, Y.C. Lin, Manipulating the generation of Ca-alginate  
520 microspheres using microfluidic channels as a carrier of gold nanoparticles, *Lab Chip*, 6  
521 (2006) 954-957.
- 522 [20] T. Murakata, H. Honma, S. Nakazato, C. Kuroda, S. Sato, Control of particle size of  
523 calcium alginate gel bead by application of electric field to interface between aqueous  
524 and organic phases, *J. Chem. Eng. Jpn.* 34 (2001) 299-305.
- 525 [21] E. Rondeau, J.J. Cooper-White, Biopolymer microparticle and nanoparticle formation  
526 within a microfluidic device, *Langmuir* 24 (2008) 6937-6945.
- 527 [22] A.M. Chuah, T. Kuroiwa, I. Kobayashi, M. Nakajima, Effect of chitosan on the stability  
528 and properties of modified lecithin stabilized oil-in-water monodisperse emulsion  
529 prepared by microchannel emulsification, *Food Hyd.* 23 (2009) 600-610.
- 530 [23] S. Sugiura, M. Nakajima, H. Ushijima, K. Yamamoto, M. Seki, Preparation  
531 characteristics of monodispersed water-in-oil emulsions using microchannel  
532 emulsification. *J. Chem. Eng. Jpn.* 34 (2001) 757-765.
- 533 [24] S. Sugiura, M. Nakajima, J. Tong, H. Nabetani, M. Seki, Preparation of monodispersed  
534 solid lipid microspheres using a microchannel emulsification technique, *J. Colloid  
535 Interface Sci.*, 227 (2000) 95-103.
- 536 [25] S. Iwamoto, K. Nakagawa, S. Sugiura, M. Nakajima, Preparation of gelatin microbeads  
537 with a narrow size distribution using microchannel emulsification, *AAPS PharmSciTech.*  
538 3 (2002) 72-76.
- 539 [26] S. Sugiura, T. Kuroiwa, T. Kagota, M. Nakajima, S. Sato, S. Mukataka, P. Walde, S.  
540 Ichikawa, Novel method for obtaining homogenous giant vesicles from a monodisperse  
541 water-in-oil emulsion prepared with a microfluidic device, *Langmuir* 24 (2008) 4581-  
542 4588.

- 543 [27] S. Sugiura, M. Nakajima, S. Iwamoto, M. Seki, Interfacial tension driven monodispersed  
544 droplet formation from microfabricated channel array, *Langmuir* 17 (2001) 5562-5566.
- 545 [28] G.T. Vladisavljevic, H. Schubert, Preparation of emulsions with a narrow particle size  
546 distribution using microporous  $\alpha$ -alumina membranes, *J. Dispersion Sci. Tech.* 24  
547 (2003) 811-819.
- 548 [29] L.S.C., Wan, P.W.S. Heng, L.W. Chan, Surfactant effects on alginate microspheres, *Int.*  
549 *J. Pharm.* 103 (1994) 267-275.
- 550 [30] T. Kawakatsu, G. Tragardh, C. Tragardh, M. Nakajima, N. Oda, T. Yonemoto, The  
551 effect of the hydrophobicity of microchannels and components in water and oil phases on  
552 droplet formation in microchannel water-in-oil emulsification, *Colloids Surf. A:*  
553 *Physicochem. Eng. Aspects*, 179 (2001) 29-37.
- 554 [31] I. Kobayashi, K. Uemura, M. Nakajima, Formulation of monodisperse emulsions using  
555 submicron-channel arrays, *Colloids Surf. A: Physicochem. Eng. Aspects*, 296, (2007)  
556 285-289.
- 557 [32] J. Tong, M. Nakajima, H. Nabetani, Y. Kikuchi, Surfactant effect on production of  
558 monodispersed microspheres by microchannel emulsification method, *J. Surfactants*  
559 *Detergents* 3 (2000) 285-293.
- 560 [33] I. Kobayashi, M. Nakajima, S. Mukataka, Preparation characteristics of oil-in-water  
561 emulsions using differently charged surfactants in straight-through microchannel  
562 emulsification. *Colloids Surf. A: Physicochem. Eng. Aspects*, 229, (2003b) 33-41.
- 563 [34] M. Saito, L. Yin, I. Kobayashi, M. Nakajima, Preparation characteristics of  
564 monodispersed oil-in-water emulsions with large particles stabilized by proteins in  
565 straight-through microchannel emulsification, *Food Hyd.* 9 (2005) 745-751.

- 566 [35] S. Sugiura, N. Kumazawa, S. Iwamoto, T. Oda, M. Satake, M. Nakajima, Effect of  
567 physical properties on droplet formation in microchannel emulsification, *Kagaku*  
568 *Kogaku Ronbunshu*, 30 (2004)129-134 (in Japanese).
- 569 [36] I. Kobayashi, S. Mukataka, M. Nakajima, Effects of type and physical properties of oil  
570 phase on oil-in-water emulsion droplet formation in straight-through microchannel  
571 emulsification, experimental and CFD studies, *Langmuir*, 21 (2005) 5722-5730.
- 572 [37] I. Kobayashi, Y. Murayama, T. Kuroiwa, K. Uemura, M. Nakajima, Production of  
573 monodisperse water-in-oil emulsions consisting of highly uniform droplets using  
574 asymmetric straight-through microchannel arrays. *Microfluid Nanofluid*, doi:  
575 10.1007/s10404-008-0368-3 (2008) (in press).
- 576 [38] V.I. Uricanu, M.H.G. Duits, D. Filip, R.M.F. Nelissen, W.G.M. Agterof, Surfactant-  
577 mediated water transport at gelatin/oil interfaces, *J. Colloid Interface Sci.* 298 (2006)  
578 920-934.
- 579 [39] P. Becher (1957), Creaming, inversion and demulsification, In *Emulsion: Theory and*  
580 *Practice*, edited by Maruzen Asian, Reinhold Publishing Corp., New York, pp. 134-165.
- 581 [40] F. Opawale, D. Burgess, Influence of interfacial properties of lipophilic surfactants on  
582 water-in-oil emulsion stability, *J. Colloid Interface Sci.* 197 (1998) 142-150.
- 583 [41] G.T. Vladisavljevic, I. Kobayashi, M. Nakajima, Generation of highly uniform droplets  
584 using asymmetric microchannels fabricated on a single crystal silicon plate: Effect of  
585 emulsifier and oil types, *Powder Tech.* 183 (2008) 37-45.
- 586 [42] I. Kobayashi, S. Mukataka, M. Nakajima, Production of monodisperse oil-in-water  
587 emulsions using a large silicon straight-through microchannel plate, *Ind. Eng. Chem.*  
588 *Res.* 44 (2005) 5852-5856.

589 [43] L.S.C., Wan, P.W.S. Heng, L.W. Chan, Development of alginate microcapsules by  
590 emulsification, Proceedings of the NUS-JSPS Seminar on Recent Developments in  
591 Pharmaceutics and Pharmaceutical Technology (1990) 243-255.

592 [44] L.S.C., Wan, P.W.S. Heng, L.W. Chan, Influence of hydrophile-lipophile balance on  
593 alginate microspheres, Int. J. Pharm. 95 (1993) 77-83.

594 [45] P.A. Williams, G.O. Phillips, The use of hydrocolloids to improve food texture, in: B.M.  
595 McKenna (Ed.), Texture in Foods, Volume 1: Semi-Solid Foods, CRC Press, Boca  
596 Raton, FL, 2003, pp. 251-274.

597 [46] A. Martinsen, G. Skjåk-Bræk, O. Smidsrød, Alginate as immobilization material: I.  
598 Correlation between chemical and physical properties of alginate beads. Biotech. Bioeng.  
599 33 (1989) 79–89.

600

601

602

603

604

605

606

607

608

609

610

611

612

613

614 **FIGURE CAPTIONS**

615 Fig. 1 (a) Microchannel emulsification experimental set-up. (b) Schematic diagram of the  
616 surface view and dimensions of CMS 6-1 silicon MC plate. (c) Schematic diagram of the  
617 flow in the MC module.

618 Fig. 2 Microscopy image of droplet formation from the grooved microchannel plate at an  
619 alginate concentration of 3 wt%. The flow rates of the dispersed and continuous phases  
620 during MC emulsification were 0.05 and 5 mL/h, respectively.

621 Fig. 3 Effects of alginate concentration in the dispersed phase on the produced water-in-oil  
622 emulsions: (a) mean droplet diameters ( $d_{av}$ ) and coefficient of variations (CV) and (b) droplet  
623 size distributions. The flow rates of the continuous and disperse phases during MC emulsion  
624 were 5 and 0.05 mL/h, respectively.

625 Fig. 4 (a) Microscopy image of droplet formation from the grooved microchannel plate at an  
626 alginate concentration of 0.1 wt%. The magnified view shows aggregates forming small  
627 aqueous droplets surrounding the to-be-dispersed phase prior to detachment as a droplet from  
628 the channel. The flow rates of the dispersed and continuous phases during MC emulsification  
629 were 0.05 mL/h and 5 mL/h, respectively. (b) Time evolution of spontaneous emulsification  
630 for (i) 0.1 wt% (ii) 2.0 wt% alginate concentration/iso-octane system with 5 wt% Span 85.

631 Fig. 5 Effects of dispersed phase flow rates on the produced water-in-oil emulsions: (a) mean  
632 particle diameters ( $d_{av}$ ) and coefficient of variations (CV), (b) particle size distributions and  
633 (c) droplet formation rate. Alginate concentration was prepared at 3 wt%. The flow rate of the  
634 continuous phase during MC emulsion was 5 mL/h.

635 Fig. 6 (a) Effect of surfactant ratio (Tween 85: Span 85) on the microscopy images of  
636 alginate microspheres (i) original water-in-oil emulsion (before external gelation) (ii) 0:1 (iii)

637 0.5:1 (iv) 1:1 (b) Particle size distribution of (i) original water-in-oil emulsion (before  
638 external gelation) (ii) alginate microspheres after external gelation prepared at alginate  
639 concentration of 3 wt%, dispersed phase flow rate of 0.05 mL/h and continuous phase flow  
640 rate of 5 mL/h. Alginate microspheres were dispersed in Milli-Q water except for the water-  
641 in-oil emulsion droplets which were dispersed in 5 wt% Span 85 in iso-octane.

642

Figure 1a&b

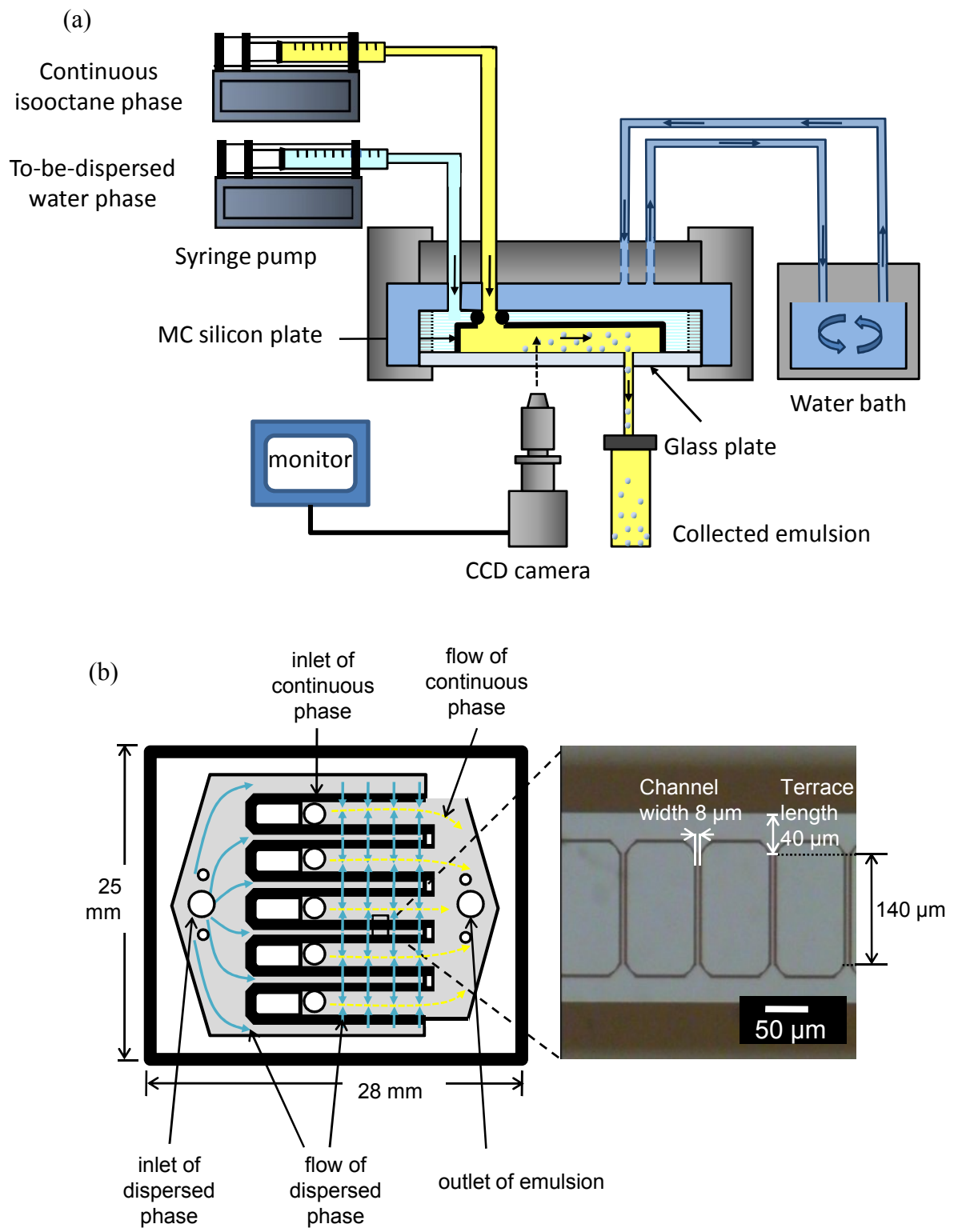


Fig. 1 Chuah et al.

Figure 1c

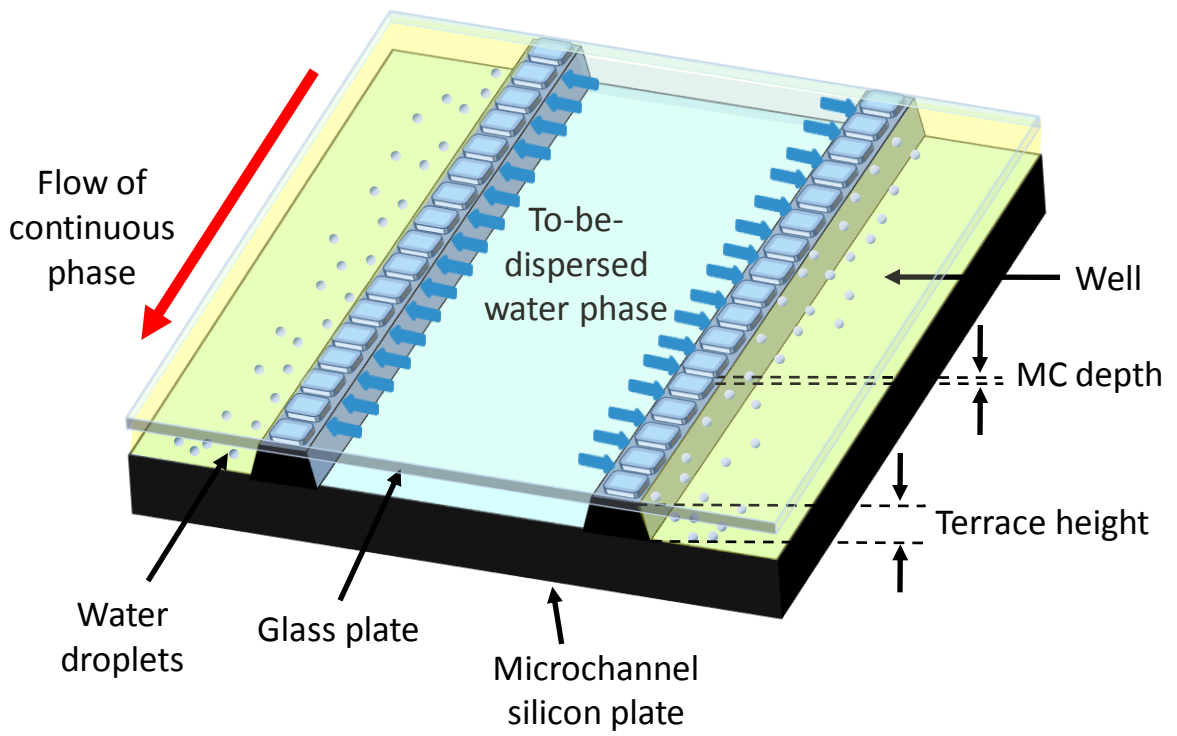


Fig. 1c

Chuah et al.

Figure 2

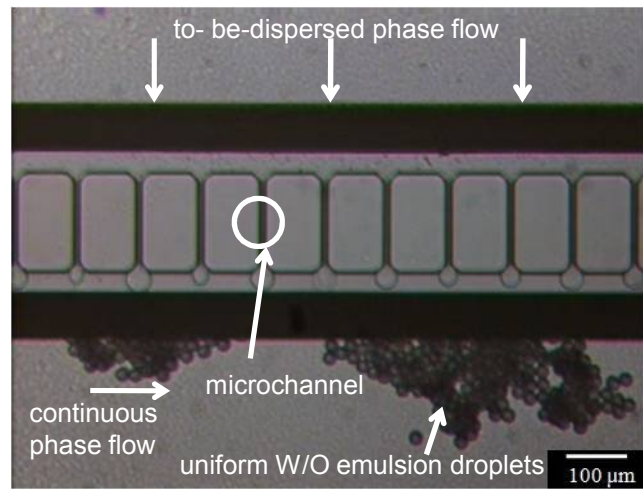


Fig. 2

Chuah et al.

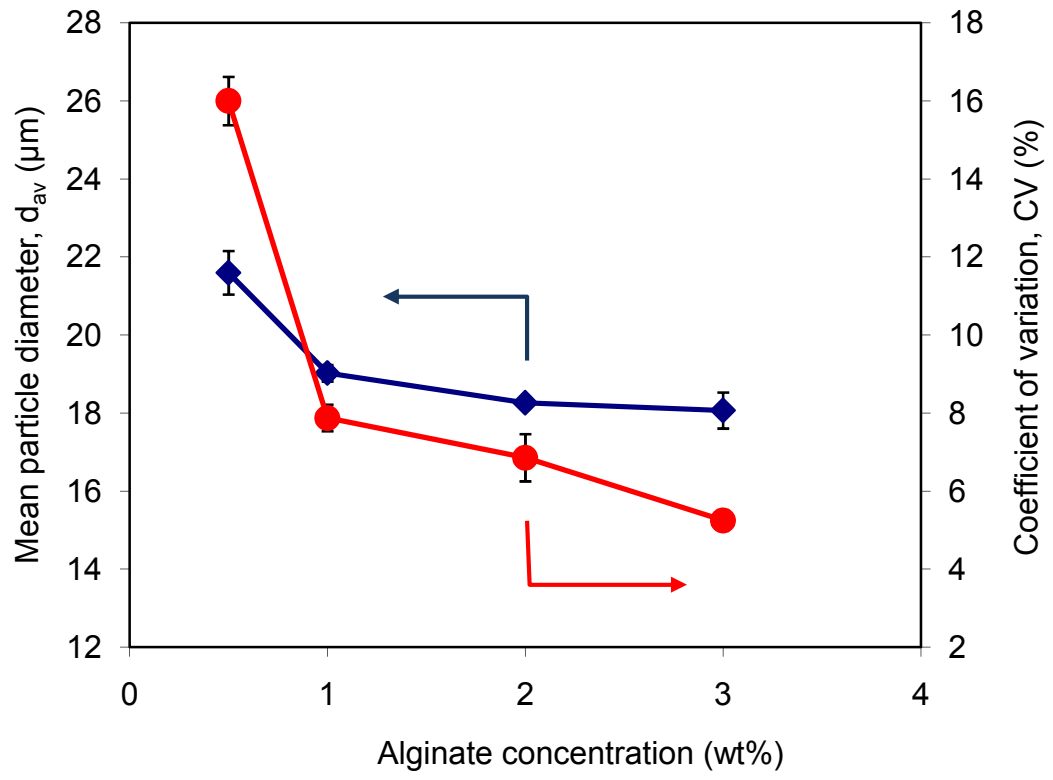


Fig. 3a

Chuah et al.

Figure 3b

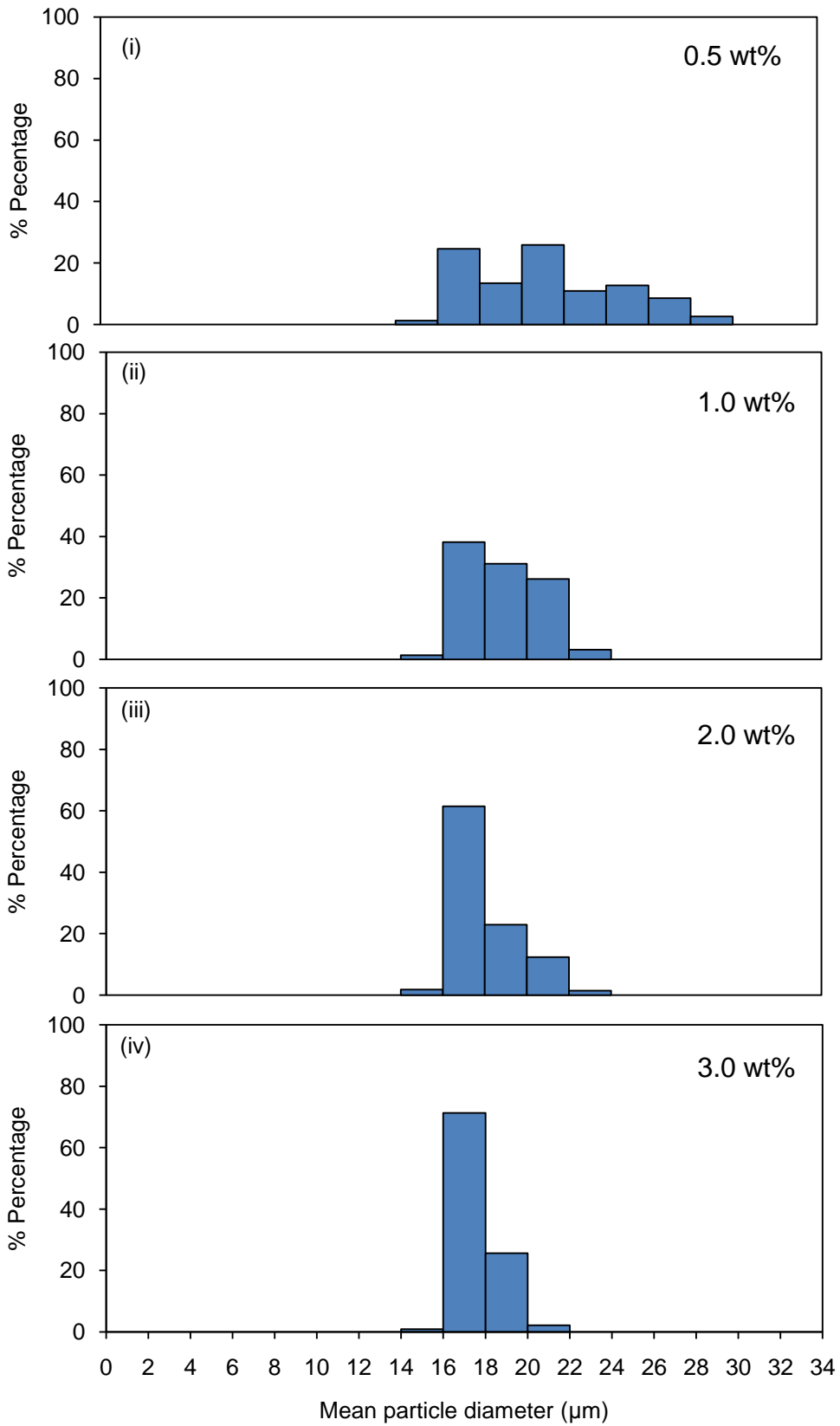


Fig. 3b

Chuah et al.

Figure 4a

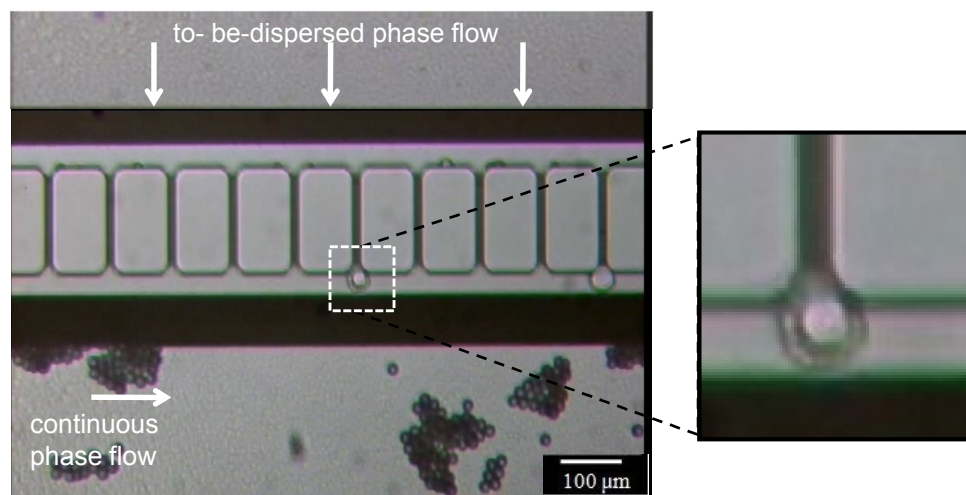
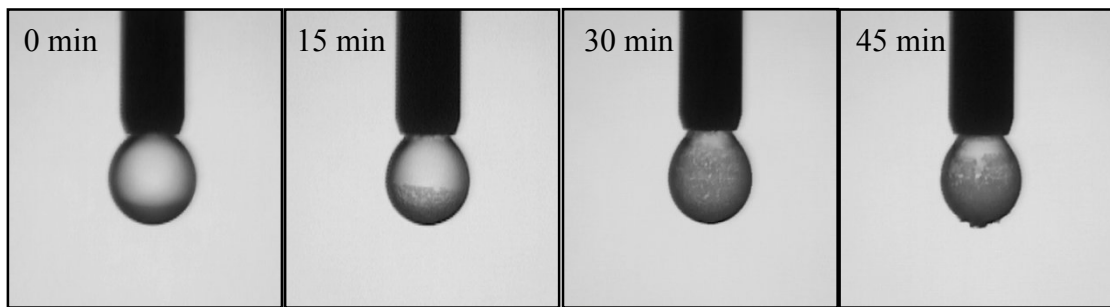


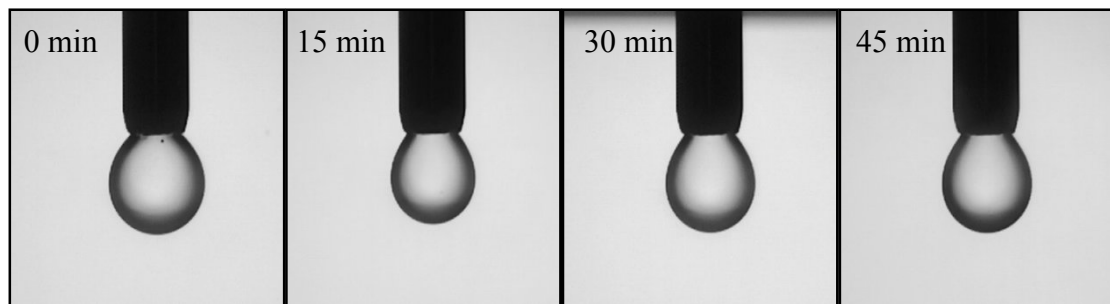
Fig. 4a Chuah et al.

(i) 0.1 wt% alginate concentration



1 mm

(ii) 2.0 wt% alginate concentration



1 mm

Fig. 4b Chuah et al.

Figure 5a

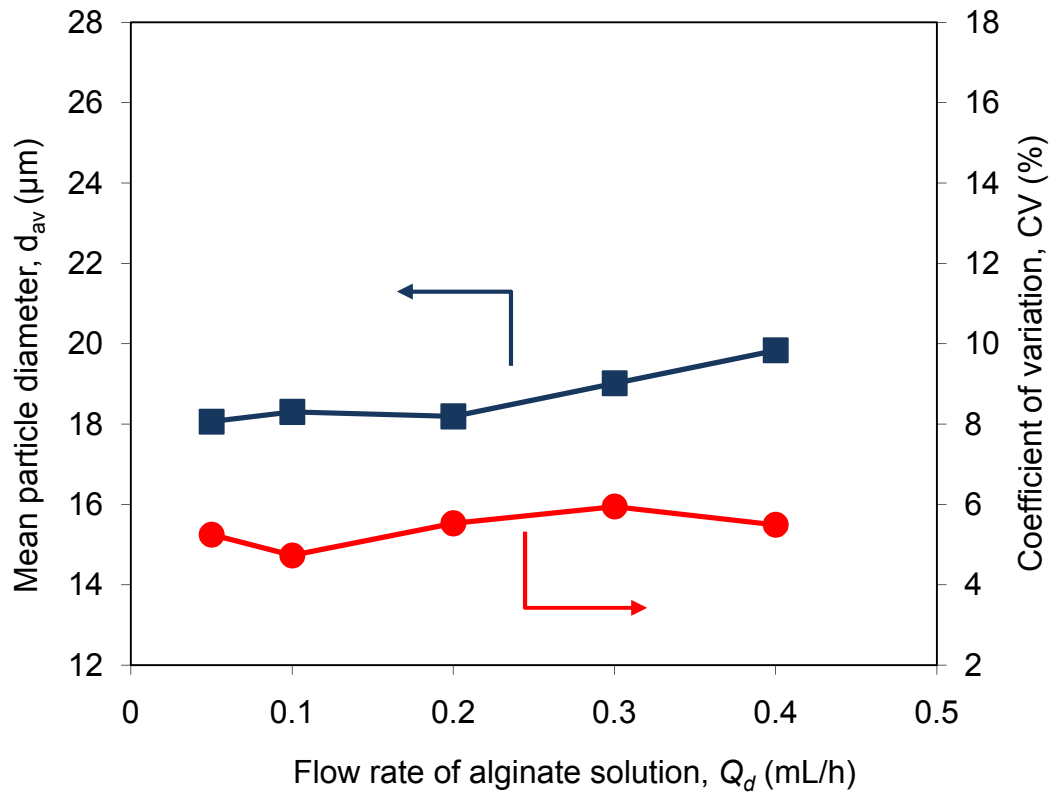


Fig. 5a

Chuah et al.

Figure 5b

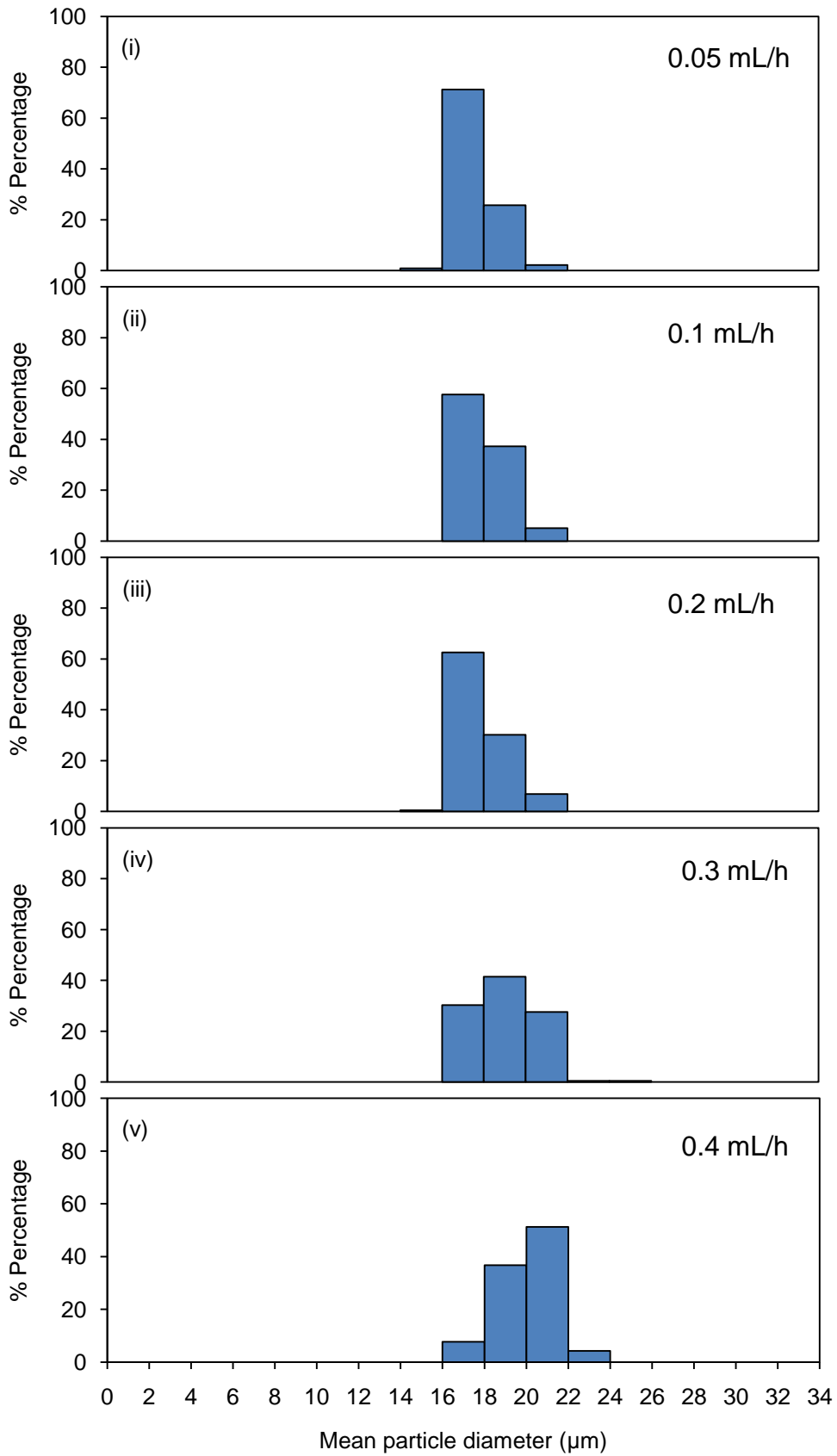


Fig. 5b

Chuah et al.

Figure 5c

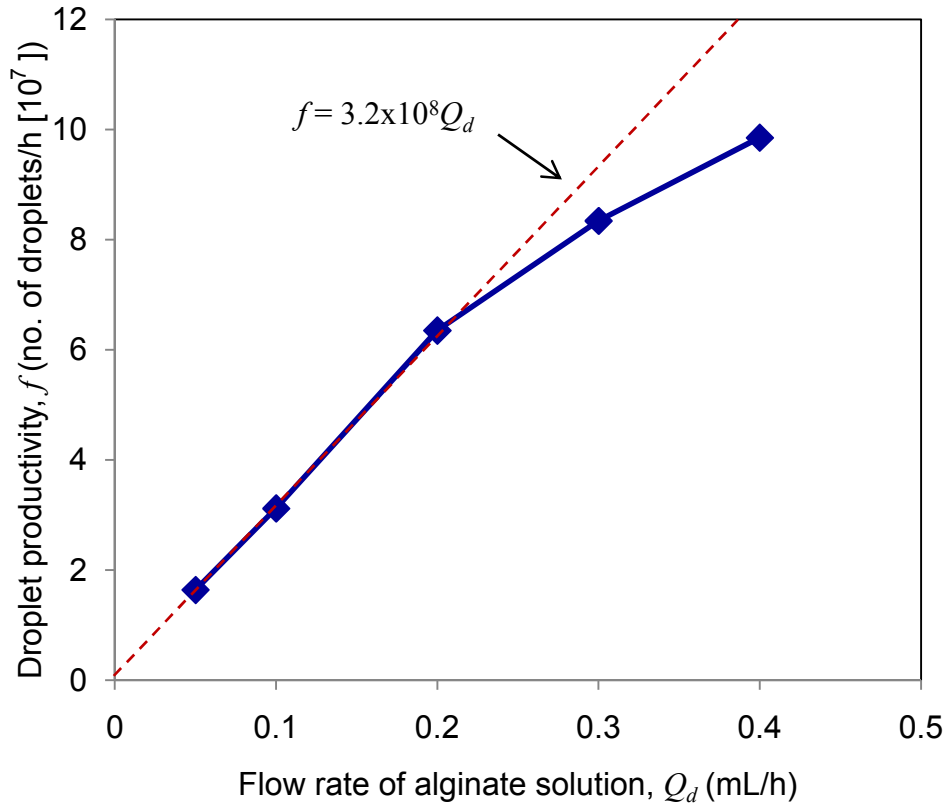


Fig. 5c

Chuah et al.

Figure 6a

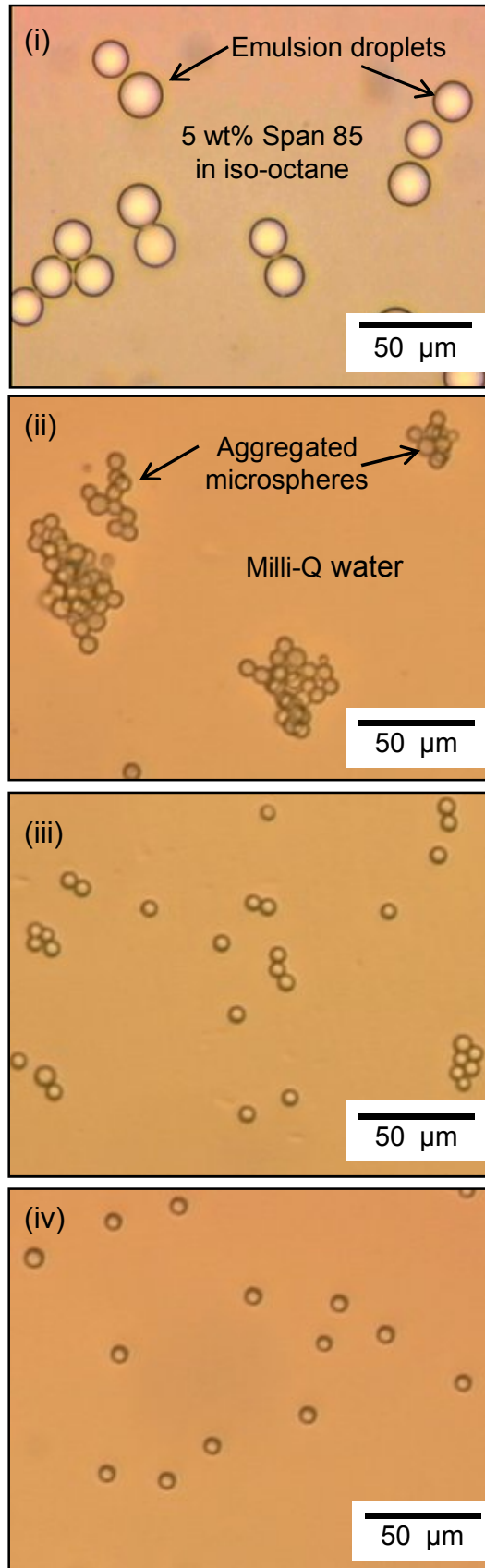


Fig. 6a

Chuah et al.

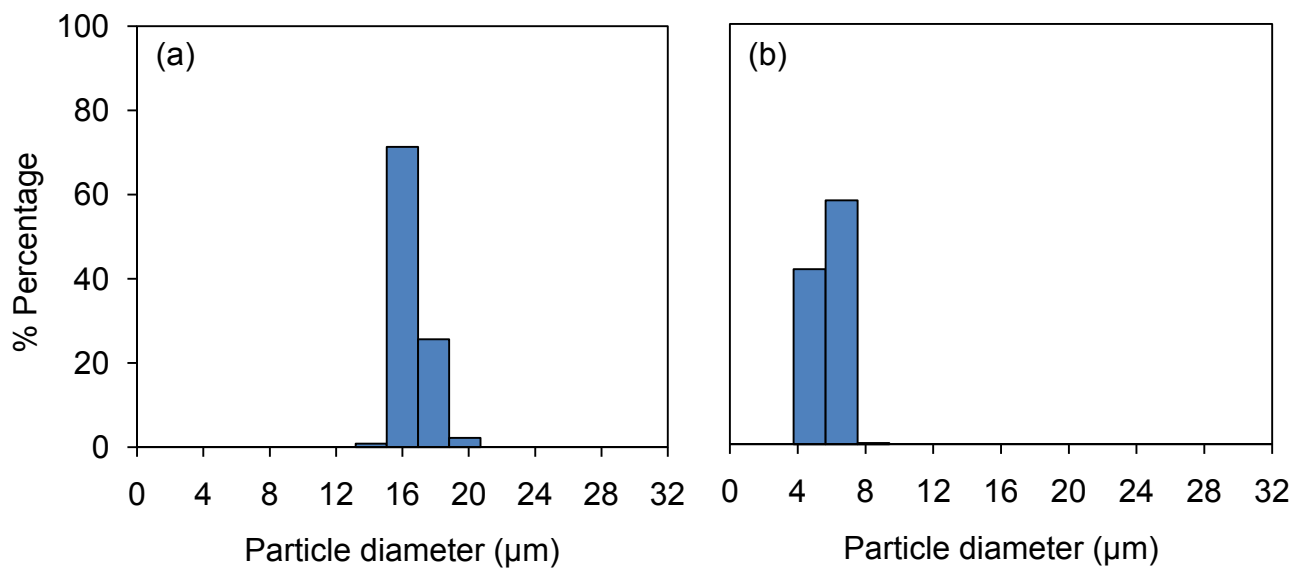


Fig. 6b

Chuah et al.

Table 1

Viscosity of alginate solutions, interfacial tension and static contact angle of the experimental system used in this study

Concentration (wt%)	Viscosity, $\eta^a$ (mPa.s)	Interfacial tension, $\gamma$ (mN/m)	Static contact angle, $\theta$ ( $^\circ$ )
Dispersed phase (Alginate solution)			
0	0.86	6.7	146.5
0.1	3.49	6.5	149.6
0.5	14.2	6.3	146.2
1.0	47.1	5.6	145.3
2.0	239	5.2	145.1
3.0	658	4.0	148.4
Continuous phase (Span 85 in iso-octane)			
5.0	0.43	-	-

<sup>a</sup> Referred to as absolute viscosity. Measured at 25 $^\circ$ C by means of a vibrational viscometer.